Letter

Paramagnetism in spherically confined charged active matter

Balázs Németh [*] and Ronojoy Adhikari [†]
Department of Applied Mathematics and Theoretical Physics, Centre for Mathematical Sciences, University of Cambridge, Wilberforce Road, Cambridge CB3 0WA, England, United Kingdom

(Received 1 February 2025; accepted 13 May 2025; published 17 June 2025)

The celebrated theorem of Bohr and van Leeuwen guarantees that a classical charged system cannot have a magnetization in thermal equilibrium. Quantum mechanically, however, a *diamagnetic* response is obtained. In contrast, we show here that a classical charged active system, consisting of a motile particle confined to the surface of a sphere, has a nonzero magnetization and a *paramagnetic* response. We numerically sample Langevin trajectories of this system and compare with limiting analytical solutions of the Fokker-Planck equation, at small and large temperatures, to find excellent agreement in the magnetic response. Our Letter suggests experimental routes to controlling and extracting work from charged active matter.

DOI: 10.1103/ccv9-c322

Introduction. The understanding that the net magnetization in a classical system of charges in equilibrium must be zero can be traced to the work of Bohr and van Leeuwen (BvL), who established this result by a consistent application of classical electrodynamics and statistical mechanics [1,2]. Peierls referred to this as a "surprise" in theoretical physics, as it required delicate cancellations of boundary currents only revealed through a dynamical analysis [3]. Landau showed, however, that by quantizing the motion of the charge a *diamagnetic* response could be obtained [4].

While the theorem of BvL rules out the possibility of magnetization in a classical system in equilibrium, it is silent on its magnetic response out of equilibrium. To drive a system out of equilibrium requires a flux of energy that can be supplied externally (as in a driven system) or internally (as in an active system). For a particle system, both drive and activity can be encoded through forces that, typically, lead to motility. A motile particle carrying a charge will produce a spontaneous electric current. It is of both theoretical and practical interest to ask if such microscopic active currents can add coherently at finite temperatures to produce a macroscopic magnetization.

To answer this question theoretically, it is desirable to focus on a system that is compact and without boundary. Compactness ensures that a nonequilibrium stationary state (NESS) can be reached, while the absence of a boundary removes the need to study the "surprising" effects of boundary currents. The obvious geometry satisfying these desiderata is the surface of a sphere. It has the additional advantage of being easily realizable in experiment, for instance by confining a charged motile particle to the surface of a liquid drop [5]. The facility of this geometry for theoretical analysis has already been established [6,7].

In this Letter we consider the Langevin dynamics of a charged particle confined to a spherical interface in a uniform magnetic field and driven out of equilibrium by an active force that is constant in its body frame. This requires both position and orientation for the description of motion. We include, correspondingly, translational and rotational inertia of the particle. The velocity dependence of the Lorentz force requires us to retain the translational velocity as a dynamical variable [8,9]. It is symmetrical to also retain the angular velocity as a dynamical variable. This allows us to formulate the dynamics geometrically in the phase space $G \times \mathfrak{g}$, where G is the Lie group of proper rotations and $\mathfrak{g}$ is its Lie algebra. This also enables noise to be added rigorously in the presence of constraints, avoids the Ito-Stratonovich dilemma, and facilitates the accurate geometric numerical sampling of Langevin trajectories.

We confirm analytically that the magnetization vanishes at zero activity for all temperatures, as expected from the equilibrium considerations of BvL. In the presence of activity, the system reaches a NESS. From the numerical sampling of trajectories, we find a nonzero net magnetization in the direction of the applied field. This is confirmed by perturbative analytical calculations at low and high temperatures. Strikingly, the induced magnetization is *paramagnetic*, in contrast to the *diamagnetic* response obtained quantum mechanically in the absence of activity. The magnetization is produced by stochastically stable Amperian loops of a given handedness that concentrate near the equator at low temperatures. We now describe our results in detail.

Kinematics. We model the active particle as a rigid body of size a, the center of mass of which is located at $\boldsymbol{r}$ and the principal axes of inertia of which are the orthonormal triad of frame vectors $\boldsymbol{e}_i$ with $i = 1, 2, 3$. The particle is constrained to move on the surface of a sphere $\mathcal{S}$ of radius R with its

[*] Contact author: bn273@cam.ac.uk
[†] Contact author: ra413@cam.ac.uk

Published by the American Physical Society under the terms of the Creative Commons Attribution 4.0 International license. Further distribution of this work must maintain attribution to the author(s) and the published article's title, journal citation, and DOI.

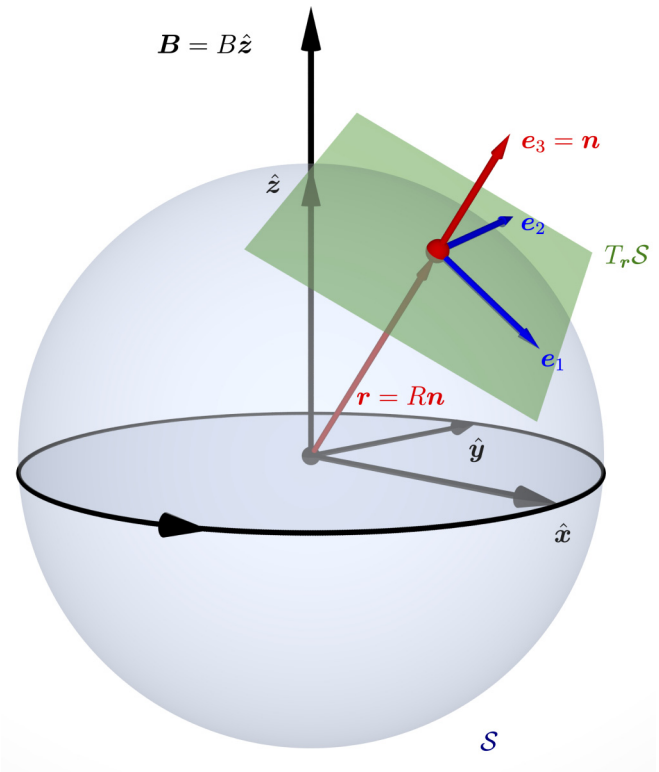


FIG. 1. A charged active particle at position $\boldsymbol{r}$ is confined to a sphere $\mathcal{S}$ of radius R in a uniform magnetic field $\boldsymbol{B} = B\hat{z}$. An orthonormal body frame $(\boldsymbol{e}_1, \boldsymbol{e}_2, \boldsymbol{e}_3)$ is rigidly attached to the particle, with $\boldsymbol{e}_3$ normal to the sphere. The velocity of the particle is in the plane T_rS tangent to S at the point $\boldsymbol{r}$ and its angular velocity is along $\boldsymbol{e}_3$. The configuration space is the Lie group $G = SO(3)$ and the phase space is $G \times \mathfrak{g}$, where $\mathfrak{g}$ is the Lie algebra of G. The solid line shows a right-handed equatorial Amperian current loop.

$\boldsymbol{e}_3$ axis pointing along the outward normal $\boldsymbol{n}$ of the sphere. Since $\boldsymbol{e}_3$ is normal to the sphere, the vectors $\boldsymbol{e}_1$ and $\boldsymbol{e}_2$ span the tangent plane $T_r\mathcal{S}$ and provide a moving frame for resolving vectors (see Fig. 1). The velocity $\boldsymbol{v}$ and the angular velocity $\boldsymbol{\Omega}$, defined by $d\boldsymbol{r} = \boldsymbol{v}dt$ and $d\boldsymbol{e}_i = (\boldsymbol{\Omega}dt) \times \boldsymbol{e}_i$, are resolved in the moving frame as $\boldsymbol{v} = v_i\boldsymbol{e}_i$ and $\boldsymbol{\Omega} = \Omega_i\boldsymbol{e}_i$, where repeated indices are summed. The motional constraints are implemented by setting $v_3 = 0$ (no normal translation) and $\boldsymbol{r} \equiv R\boldsymbol{n} = R\boldsymbol{e}_3$ (no independent rotation about an axis in the tangent plane). The particle configuration, then, is fully contained in the three frame vectors. From the rotational constraint it follows that $d\boldsymbol{r} = Rd\boldsymbol{e}_3 = R(\boldsymbol{\Omega}dt) \times \boldsymbol{e}_3$ and so $\boldsymbol{v} = R\boldsymbol{\Omega} \times \boldsymbol{e}_3$, showing that the tangential components of the angular velocity and the translational velocity are mutually dependent. This leaves three independent kinematic degrees of freedom, which we take to be the two components of translational velocity v_1 and v_2 and the single component of angular velocity $\omega \equiv \Omega_3$, all expressed in the body frame. Since the motion of the frame is an orthogonal transformation, the configuration space can be identified with the special orthogonal group $G = SO(3)$. The infinitesimal change in the frame $\boldsymbol{\Omega}dt$ is then naturally identified with the Lie algebra $\mathfrak{g} = \mathfrak{so}(3)$ of infinitesimal rotations. The dynamical phase space is $G \times \mathfrak{g}$. The *constrained* motion of the particle can thus be described by the *unconstrained* motion of its body frame. This offers significant advantages in formulating the equations of motion as we show below [10].

Deterministic dynamics. We immerse the system above in a uniform magnetic field $\boldsymbol{B} = B\hat{z}$ with a corresponding vector potential $\boldsymbol{A}$, such that $\boldsymbol{B} = \nabla \times \boldsymbol{A}$. The particle has mass m and moment of inertia J along the $\boldsymbol{e}_3$ axis. The deterministic dynamics is most easily formulated in terms of the Lagrangian $L = \frac{1}{2}m\boldsymbol{v} \cdot \boldsymbol{v} + \frac{1}{2}J\omega^2 + q\boldsymbol{A} \cdot \boldsymbol{v}$, which includes translational and rotational kinetic energies and the coupling to the magnetic field. We vary this Lagrangian maintaining the orthogonality of the frame vectors and respecting the velocity constraints to obtain the conservative dynamics [11,12]. To this we add an active force $\boldsymbol{F}_A = F_A\boldsymbol{e}_1$ that is constant in the body frame and acts along the first principal axis, frictional forces proportional to the velocities and a frictional torque proportional to the angular velocity. The resulting equations are

$$m\dot{v}_1 = +\Big(\Delta m\omega + m\omega_c\frac{z}{R}\Big)v_2 - \gamma_T v_1 + F_A, \tag{1}$$

$$m\dot{v}_2 = -\Big(\Delta m\omega + m\omega_c\frac{z}{R}\Big)v_1 - \gamma_T v_2, \tag{2}$$

$$J\dot{\omega} = -\gamma_R\omega, \quad \omega_c = \frac{qB}{m}, \tag{3}$$

$$\dot{\boldsymbol{e}}_i = \boldsymbol{\Omega} \times \boldsymbol{e}_i, \quad \boldsymbol{e}_3 = \frac{\boldsymbol{r}}{R}, \tag{4}$$

where $\Delta m = m(1 - \frac{J}{mR^2})$ is an effective mass, ω_c is the cyclotron frequency, and γ_T (γ_R) is the translational (rotational) friction coefficient. Since $J \sim ma^2$, we can neglect the correction to the mass for a small particle on a large sphere ($a \ll R$) and set $\Delta m = m$. Our results do not change qualitatively by making this approximation. Then, the conservative part of the above dynamics rotates velocities at a rate $\varpi = \omega + \omega_c z/R$ and conserves the angular velocity ω. These Hamiltonian orbits, shown in Fig. 2(a), are similar to those of a symmetric top but show a precession about the axis of the external magnetic field. With friction and activity, the Hamiltonian orbits are attracted to a limit cycle at the equator with $v_1 = F_A/\gamma_T \equiv u$, $v_2 = 0$ and $\omega = 0$, as shown in Fig. 2(b). The equatorial limit cycles are reminiscent of traveling bands of active particles around geodesics reported in earlier studies of many interacting active agents on spheres [13,14]. There, a stable equatorial orbit is chosen through a spontaneous and collective many-particle breaking of symmetry, while here the external magnetic field breaks symmetry and selects the stable equatorial orbit even at the one-particle level.

The limit cycle results in an Amperian loop carrying a current $qu/2\pi R$ and enclosing a planar area πR^2 which produces a magnetic moment $\mu_a = quR/2$ in the z direction. The moment is parallel to the applied field and hence the response is paramagnetic. Thus, the interplay of an applied magnetic field, activity, friction, and confinement yields an activity-induced realization of a classical magnetic spin. How does this effective spin behave at finite temperatures?

Stochastic dynamics. To answer this question we promote our deterministic equations of motion to Langevin equations by adding noise that obeys the fluctuation-dissipation relation (FDR). This is in contrast to [15], where the authors find a nonzero magnetization in a NESS obtained

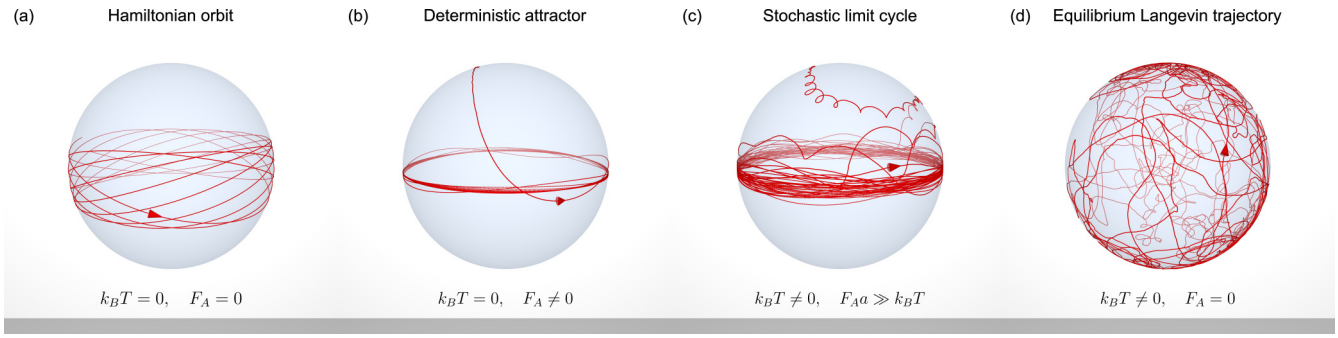


FIG. 2. (a)–(d) Typical trajectories of deterministic ($k_BT = 0$) and stochastic ($k_BT \neq 0$) dynamics for magnetic field B and activity F_A. (a) Hamiltonian orbits for $k_BT = F_A = 0$ and zero friction $\gamma_T = \gamma_R = 0$. (b) Deterministic attractor for $k_BT = 0$. (c) Stochastic limit cycle at low temperatures with $k_BT \ll F_A a$. The deterministic attractor is stochastically stable at low temperatures and trajectories in (c) contribute to a nonzero paramagnetic response. (d) Equilibrium Langevin trajectories $k_BT \neq 0$, $F_A = 0$ on the sphere. See movie in Supplemental Material [11] for animations of the dynamics.

by violating the FDR. To make contact with statistical mechanics, we introduce the probability measure in phase space $p(\boldsymbol{e}_i, \boldsymbol{\Omega}, t)dgd\boldsymbol{\Omega}$, where dg is the invariant volume element in G and $d\boldsymbol{\Omega} = dv_1 dv_2 d\omega$ is the volume element in $\mathfrak{g}$. The time evolution of the probability density $p(\boldsymbol{e}_i, \boldsymbol{\Omega}, t)$ is governed by the Fokker-Planck equation $\partial_t p = \mathcal{L}p$, derived from the Langevin equations via standard methods [16]. The resulting Fokker-Planck operator $\mathcal{L}$ is [11]

$$\mathcal{L} = \frac{v_2}{R}L_1 - \frac{v_1}{R}L_2 - \omega L_3 + \varpi\left(\boldsymbol{v}\times\frac{\partial}{\partial \boldsymbol{v}}\right) + \frac{\gamma_T}{m}\frac{\partial}{\partial \boldsymbol{v}}\boldsymbol{v} + \frac{\gamma_R}{J}\frac{\partial}{\partial\omega}\omega - \frac{F_A}{m}\frac{\partial}{\partial v_1} + \frac{k_BT\gamma_T}{m^2}\frac{\partial^2}{\partial \boldsymbol{v}^2} + \frac{k_BT\gamma_R}{J^2}\frac{\partial^2}{\partial\omega^2}. \quad (5)$$

The L_i above are generators of infinitesimal rotations about the frame vectors $\boldsymbol{e}_i$. They are left-invariant vector fields in G and are related to angular momentum operators in quantum mechanics. The shorthand notations $\boldsymbol{v}\times\frac{\partial}{\partial \boldsymbol{v}} = v_1\frac{\partial}{\partial v_2} - v_2\frac{\partial}{\partial v_1}$, $\frac{\partial}{\partial \boldsymbol{v}}\boldsymbol{v} = \frac{\partial}{\partial v_1}v_1 + \frac{\partial}{\partial v_2}v_2$, and $\frac{\partial^2}{\partial \boldsymbol{v}^2} = \frac{\partial^2}{\partial v_1^2} + \frac{\partial^2}{\partial v_2^2}$ are used for brevity. The use of the body frame and the phase space $G\times\mathfrak{g}$ yields a Fokker-Planck operator that is invariant under choice of local coordinates. The subtle issues of adding noise to degrees of freedom constrained to remain on manifolds (G is an orthogonal matrix group) are obviated by adding noise to their velocities (which are unconstrained in the matrix Lie algebra $\mathfrak{g}$). This also removes room for Ito-Stratonovich ambiguities. Langevin trajectories can be sampled by splitting the Fokker-Planck operator into the conservative Hamiltonian drift and an Ornstein-Uhlenbeck drift diffusion in the space of angular velocities. Each of these can be sampled efficiently and accurately [17,18]. The splitting method converges with a weak order of 2 and respects the spherical confinement of the position and orthogonality of the body frame. The magnetic moment is calculated from the average $\boldsymbol{\mu} = (q/2)\langle \boldsymbol{r}\times\boldsymbol{v}\rangle_{\rm SS}$ with respect to the steady state probability measure, either analytically or from numerically sampled trajectories. By symmetry, $\boldsymbol{\mu}$ can only have a nonzero component in the z direction. We, therefore, confine attention to the rescaled magnetic moment $\mu \equiv (\boldsymbol{\mu}\cdot\hat{\boldsymbol{z}})/\mu_a$ and study its variation with the temperature and magnetic field.

Thermal equilibrium. We assume that the dynamics relaxes to a unique stationary state $p_{\rm SS}(\boldsymbol{e}_i, \boldsymbol{\Omega})$ as $t\to\infty$ which satisfies $\mathcal{L}p_{\rm SS} = 0$. In the presence of the magnetic field but in the absence of activity it is easy to verify by substitution that the Gibbs distribution,

$$p^{\rm eq}_{\rm SS}(\boldsymbol{e}_i, \boldsymbol{\Omega}) = \sqrt{\frac{m^2J}{(2\pi k_BT)^3}}\exp\left(-\frac{m\boldsymbol{v}^2 + J\omega^2}{2k_BT}\right),$$

is the stationary solution. This shows that $\boldsymbol{r}$ and $\boldsymbol{v}$ are independently distributed in equilibrium and it immediately follows that $\boldsymbol{\mu}^{\rm eq} = (q/2)(\langle\boldsymbol{r}\rangle^{\rm eq}\times\langle\boldsymbol{v}\rangle^{\rm eq}) = 0$. This verifies the BvL theorem and confirms, through an independent analysis, that there is no magnetization in equilibrium in a spherical geometry [6,7]. We now turn to dynamics with activity.

Low temperatures and strong magnetic fields. Since solving the Fokker-Planck equation analytically is no longer possible in the presence of activity, we first examine the low-temperature limit, asking if the equatorial attractor is stable to noise. We use a van Kampen expansion [19] to obtain an Ornstein-Uhlenbeck process for small perturbations about the attractor. We find the attractor to be stable to small noise and consequently the Amperian loops, now stochastic, add coherently to produce a nonzero magnetic moment. In the limit of vanishing rotational inertia, we obtain to leading order in k_BT [11]

$$\mu \approx 1 - \frac{k_BT}{quRB}. \quad (6)$$

This magnetic response is identical to the low-temperature limit of a classical spin of magnetic moment μ_a in a constant magnetic field of magnitude B in thermal equilibrium. The average magnetic moment μ_a is reduced by an amount proportional to k_BT due to Gaussian fluctuations of the spin about the direction of the field. The numerical sampling of trajectories confirms this analytical result. Typical low-temperature trajectories, shown in Fig. 2(c), remain confined near the attractor with $\langle z\rangle = 0$ and $\langle z^2\rangle = k_BTR/qBu$. The appearance of B in the denominator of the expression for μ and $\langle z^2\rangle$ shows that in order to have a substantial magnetic moment and a stable equatorial orbit, we need both low temperatures and strong fields. These ensure a strongly attracting equatorial limit cycle. The average magnetic moment computed from the trajectories agrees very well with the analytical approxima-

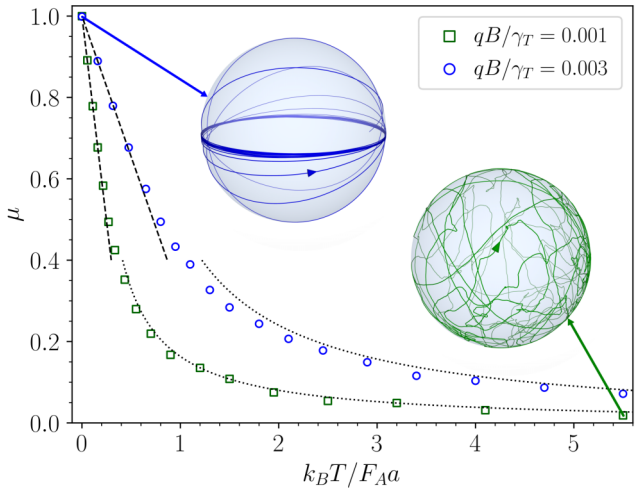


FIG. 3. Magnetic moment μ as a function of temperature for fixed activity and magnetic field. For low temperatures, the magnetic moment is a linear function of temperature with intercept 1, while for high temperatures it decays as $1/k_BT$. The two limiting regimes are separated by an intermediate region where $k_BT \sim quRB$. The analytical predictions for the slope of the linear regime and the rate of decay, shown as the dashed and dotted curves, respectively, agree well with the numerical results. The insets corresponding to data points with blue and green trajectories show low- and high-temperature orbits, respectively. Error bars are bounded by the sizes of the markers. As the limit of zero rotational inertia is inaccessible in our simulations, we have used the results of the perturbative calculations at finite rotational inertia [11].

tions as shown in Fig. 3. From Eq. (6) we see that thermal fluctuations are significant for $k_BT \sim quRB$.

High temperatures and weak magnetic fields. Having established a nonzero magnetization in the NESS at low temperatures and high fields, we ask how robust this effect is to an increase in temperature or a weakening of the field. This requires an involved calculation setting up the Brinkman hierarchy [20] for the Fokker-Planck operator (5) and applying a closure. Again in the limit of vanishing rotational inertia, we obtain to leading order in $1/k_BT$ and B [11]

$$\mu \approx \frac{quRB}{3k_BT}. \tag{7}$$

The dependence of the magnetic moment on the magnetic field and temperature is reminiscent of Curie's law in classical paramagnetism [21,22].

Irreversibility. We now provide a trajectorial interpretation of the nonzero magnetic moment. Assuming that the stochastic dynamics is ergodic, we can write the steady state magnetic moment as a long-time average of the path-dependent observable:

$$\mu = \frac{\hat{z}}{\mu_a} \cdot \left[\lim_{t\to\infty} \frac{q}{2t} \int_0^t (\boldsymbol{r} \times \boldsymbol{v}) dt \right] \tag{8a}$$

$$= \frac{1}{\mu_a} \left[\lim_{t\to\infty} \frac{q}{2t} \int_{\mathcal{C}_t} (\hat{z} \times \boldsymbol{r}) \cdot d\boldsymbol{r} \right] \tag{8b}$$

$$\propto \lim_{t\to\infty} \frac{1}{t} \int_{\mathcal{C}_t} \boldsymbol{A} \cdot d\boldsymbol{r}, \tag{8c}$$

where in Eqs. (8b) and (8c), the integral is along the stochastic trajectory $\mathcal{C}_t$ of duration t. We have made a gauge choice $\boldsymbol{A}(\boldsymbol{r}) = B(\hat{z} \times \boldsymbol{r})/2$ but the result above is gauge independent. Equation (8c) shows that the steady state magnetic moment is proportional to the long-time average of the line integral of the gauge potential along the stochastic trajectory. This suggests that it is also a dynamical measure of irreversibility in the system, where detailed balance is broken by the nonconservative active force which is able to do work on the particle when going around a closed loop in configuration space. The instantaneous value of the integrand for trajectories in Fig. 2 is animated in [11]. The violation of detailed balance does not necessarily imply a nonzero magnetic moment though, as the following counterexample demonstrates. Replacing the uniform magnetic field by that of a monopole at the center of the sphere produces a NESS in which there is no breaking of symmetry and the position and the velocity remain independently distributed. The magnetic moment thus vanishes even in NESS. The subtleties of NESS in the presence of magnetic fields have been noted in [23–29].

Conclusion. We have shown that a charged active particle in a confined geometry subject to linear friction follows a geodesic that is selected by the magnetic field. This establishes an Amperian loop pointing in the direction of the magnetic field and yields a paramagnetic response at finite temperatures. This provides, both qualitatively and quantitatively, a classical realisation of spin. A possible experimental realization of our system could be based on charged nanomotors confined by capillary effects to spherical liquid-liquid interfaces, for example the interfaces of emulsion droplets [5]. For micron-sized objects $a \approx 1\,\mu\text{m}$ with swimming speed $u \approx 100\,\mu\text{m}\,\text{s}^{-1}$ [30] at room temperature $T \approx 300\,\text{K}$, assuming Stokes drag in a fluid with the viscosity of water, we find $F_Aa/k_BT \approx 500$. The relative variance of trajectories $\langle z^2/R^2 \rangle = k_BT/quRB$ can be made small by increasing the magnetic field. We thus expect the Amperian loops to be observable in room-temperature experiments.

The stability of active current loops can be harnessed to steer active charged particles using a magnetic field [31]. Our system demonstrates an alternative way to control active particles using magnetic fields via the Lorentz force compared to previous approaches relying on magnetic torques and forces on permanent magnetic moments [32–37]. The present theory will apply if changes in the steering magnetic field are slow compared to the relaxation time of the plane of the current loop to a change in direction of the magnetic field. If the changes are comparable, we can expect the transient between stationary states, not studied here, to lead to memory effects [38] and a frequency-dependent paramagnetic response [39]. The latter suggests that nonequilibrium work can be extracted from the system using suitable cyclic, and not necessarily adiabatic, time-dependent magnetic fields [31,40,41]. This further suggests interesting connections to stochastic thermodynamics and fluctuation theorems, where electromechanical effects have been noted [7,42–45]. The connections between our results and the rich phenomenology found in chiral active matter [46,47] remain to be explored. In conclusion, our Letter establishes the possibility of paramagnetism in a classical

system and reveals the surprising effects that can arise through the interplay of electromagnetic, viscous, and active forces in soft matter.

Acknowledgments. We thank Prof. M. E. Cates for insightful comments and a careful reading of the Letter and Prof. S. R. Ramaswamy for stimulating discussions. This research was supported by Engineering and Physical Sciences Research Council Grant No. EP/W524141/1 (B.N.) and in part by NSF Grant No. PHY-2309135 to the Kavli Institute for Theoretical Physics.

Data availability. The data supporting this study's findings are available within the article.

[1] N. Bohr, Studies on the electron theory of metals, in *Niels Bohr Collected Works—Volume 1—Early Work (1905–1911)*, edited by L. Rosenfeld and J. Rud Nielsen (North-Holland, Amsterdam, 1972), pp. 163–393, translation of Ph.D. thesis, University of Copenhagen, 1911.

[2] H.-J. Van Leeuwen, Problèmes de la théorie électronique du magnétisme, J. Phys. Radium **2**, 361 (1921).

[3] R. E. Peierls, *Surprises in Theoretical Physics*, Princeton Series in Physics (Princeton University, Princeton, NJ, 1979).

[4] L. Landau, Diamagnetismus der Metalle, Z. Phys. **64**, 629 (1930).

[5] W. Fei, M. M. Driscoll, P. M. Chaikin, and K. J. M. Bishop, Magneto-capillary dynamics of amphiphilic Janus particles at curved liquid interfaces, Soft Matter **14**, 4661 (2018).

[6] N. Kumar and K. Vijay Kumar, Classical Langevin dynamics of a charged particle moving on a sphere and diamagnetism: A surprise, Europhys. Lett. **86**, 17001 (2009).

[7] P. Pradhan and U. Seifert, Nonexistence of classical diamagnetism and nonequilibrium fluctuation theorems for charged particles on a curved surface, Europhys. Lett. **89**, 37001 (2010).

[8] H.-M. Chun, X. Durang, and J. D. Noh, Emergence of nonwhite noise in Langevin dynamics with magnetic Lorentz force, Phys. Rev. E **97**, 032117 (2018).

[9] H. D. Vuijk, J. M. Brader, and A. Sharma, Anomalous fluxes in overdamped Brownian dynamics with Lorentz force, J. Stat. Mech. (2019) 063203.

[10] H. Poincaré, Sur une forme nouvelle des équations de la Mécanique, C. R. Acad. Sci. **132**, 369 (1901).

[11] See Supplemental Material at http://link.aps.org/supplemental/10.1103/ccv9-c322 for derivations of theoretical results, details of numerical simulations, and a movie of the dynamics, which includes Refs. [48–52].

[12] J. E. Marsden and T. S. Ratiu, *Introduction to Mechanics and Symmetry: A Basic Exposition of Classical Mechanical Systems*, 2nd ed., Texts in Applied Mathematics Vol. 17 (Springer, New York, 2003).

[13] R. Sknepnek and S. Henkes, Active swarms on a sphere, Phys. Rev. E **91**, 022306 (2015).

[14] S. Henkes, M. C. Marchetti, and R. Sknepnek, Dynamical patterns in nematic active matter on a sphere, Phys. Rev. E **97**, 042605 (2018).

[15] M. Muhsin, M. Sahoo, and A. Saha, Orbital magnetism of an active particle in viscoelastic suspension, Phys. Rev. E **104**, 034613 (2021).

[16] C. W. Gardiner, *Stochastic Methods: A Handbook for the Natural and Social Sciences*, 4th ed., Springer Series in Synergetics Vol. 13 (Springer-Verlag, Berlin, 2009).

[17] E. Hairer, C. Lubich, and G. Wanner, *Geometric Numerical Integration: Structure-Preserving Algorithms for Ordinary Differential Equations*, Springer Series in Computational Mathematics Vol. 31 (Springer-Verlag, Berlin, 2006).

[18] S. A. Chin, Symplectic and energy-conserving algorithms for solving magnetic field trajectories, Phys. Rev. E **77**, 066401 (2008).

[19] N. G. van Kampen, *Stochastic Processes in Physics and Chemistry*, 3rd ed., North-Holland Personal Library (Elsevier, Amsterdam, 2007).

[20] H. Brinkman, Brownian motion in a field of force and the diffusion theory of chemical reactions, Physica **22**, 29 (1956).

[21] P. Langevin, Sur la théorie du magnétisme, J. Phys. Theor. Appl. **4**, 678 (1905).

[22] J. H. Van Vleck, *The Theory of Electric and Magnetic Susceptibilities* (Oxford University, New York, 1965).

[23] S. Lee and C. Kwon, Nonequilibrium driven by an external torque in the presence of a magnetic field, Phys. Rev. E **99**, 052142 (2019).

[24] H. D. Vuijk, J. U. Sommer, H. Merlitz, J. M. Brader, and A. Sharma, Lorentz forces induce inhomogeneity and flux in active systems, Phys. Rev. Res. **2**, 013320 (2020).

[25] I. Abdoli, H. D. Vuijk, R. Wittmann, J. U. Sommer, J. M. Brader, and A. Sharma, Stationary state in Brownian systems with Lorentz force, Phys. Rev. Res. **2**, 023381 (2020).

[26] I. Abdoli, E. Kalz, H. D. Vuijk, R. Wittmann, J.-U. Sommer, J. M. Brader, and A. Sharma, Correlations in multithermostat Brownian systems with Lorentz force, New J. Phys. **22**, 093057 (2020).

[27] A. Matevosyan and A. E. Allahverdyan, Nonequilibrium, weak-field-induced cyclotron motion: A mechanism for magnetobiology, Phys. Rev. E **104**, 064407 (2021).

[28] M. Muhsin and M. Sahoo, Inertial active Ornstein-Uhlenbeck particle in the presence of a magnetic field, Phys. Rev. E **106**, 014605 (2022).

[29] M. Muhsin, F. Adersh, and M. Sahoo, Active magneto gyrator: Memory-induced trapped diamagnetism, Phys. Rev. E **111**, 015411 (2025).

[30] W. Wang, L. A. Castro, M. Hoyos, and T. E. Mallouk, Autonomous motion of metallic microrods propelled by ultrasound, ACS Nano **6**, 6122 (2012).

[31] L. K. Davis, K. Proesmans, and É. Fodor, Active matter under control: Insights from response theory, Phys. Rev. X **14**, 011012 (2024).

[32] P. Tierno, R. Golestanian, I. Pagonabarraga, and F. Sagués, Controlled swimming in confined fluids of magnetically actuated colloidal rotors, Phys. Rev. Lett. **101**, 218304 (2008).

[33] P. Guillamat, J. Ignés-Mullol, and F. Sagués, Control of active liquid crystals with a magnetic field, Proc. Natl. Acad. Sci. USA **113**, 5498 (2016).

[34] P. Mandal, G. Patil, H. Kakoty, and A. Ghosh, Magnetic active matter based on helical propulsion, Acc. Chem. Res. **51**, 2689 (2018).

[35] A. F. Demirörs, M. T. Akan, E. Poloni, and A. R. Studart, Active cargo transport with Janus colloidal shuttles using electric and magnetic fields, Soft Matter **14**, 4741 (2018).

[36] K. Bente, A. Codutti, F. Bachmann, and D. Faivre, Biohybrid and bioinspired magnetic microswimmers, Small **14**, 1704374 (2018).

[37] D. Matsunaga, J. K. Hamilton, F. Meng, N. Bukin, E. L. Martin, F. Y. Ogrin, J. M. Yeomans, and R. Golestanian, Controlling collective rotational patterns of magnetic rotors, Nat. Commun. **10**, 4696 (2019).

[38] A. Théry, A. Chamolly, and E. Lauga, Controlling confined collective organization with taxis, Phys. Rev. Lett. **132**, 108301 (2024).

[39] M. Baiesi, C. Maes, and B. Wynants, Fluctuations and response of nonequilibrium states, Phys. Rev. Lett. **103**, 010602 (2009).

[40] É. Fodor and M. E. Cates, Active engines: Thermodynamics moves forward, Europhys. Lett. **134**, 10003 (2021).

[41] I. Abdoli, R. Wittmann, J. M. Brader, J.-U. Sommer, H. Löwen, and A. Sharma, Tunable Brownian magneto heat pump, Sci. Rep. **12**, 13405 (2022).

[42] A. M. Jayannavar and M. Sahoo, Charged particle in a magnetic field: Jarzynski equality, Phys. Rev. E **75**, 032102 (2007).

[43] A. Saha and A. M. Jayannavar, Nonequilibrium work distributions for a trapped Brownian particle in a time-dependent magnetic field, Phys. Rev. E **77**, 022105 (2008).

[44] J. I. Jiménez-Aquino, Work-fluctuation theorem for a charged harmonic oscillator, J. Phys. A **44**, 295002 (2011).

[45] U. Seifert, Stochastic thermodynamics, fluctuation theorems and molecular machines, Rep. Prog. Phys. **75**, 126001 (2012).

[46] E. Lauga, W. R. DiLuzio, G. M. Whitesides, and H. A. Stone, Swimming in circles: Motion of bacteria near solid boundaries, Biophys. J. **90**, 400 (2006).

[47] B. Liebchen and D. Levis, Chiral active matter, Europhys. Lett. **139**, 67001 (2022).

[48] G. A. Pavliotis, *Stochastic Processes and Applications: Diffusion Processes, the Fokker-Planck and Langevin Equations*, Texts in Applied Mathematics Vol. 60 (Springer, New York, 2014).

[49] B. Németh and R. Adhikari, Intrinsic Langevin dynamics of rigid inclusions on curved surfaces, Phys. Rev. E **111**, 045418 (2025).

[50] J. O'Byrne and M. E. Cates, Geometric theory of (extended) time-reversal symmetries in stochastic processes: I. Finite dimension, J. Stat. Mech. (2024) 113207.

[51] M. Gopal, *Control Systems: Principles and Design*, 2nd ed. (McGraw-Hill, New York, 2003).

[52] R. Czopnik and P. Garbaczewski, Brownian motion in a magnetic field, Phys. Rev. E **63**, 021105 (2001).